

### 3. RESULTS AND DISCUSSION

#### 3.1 The Effect of Boundary Conditions on Iodine Volatility

The following sections summarize some of the trends that are observed in code predictions of the percentage of the iodine inventory in the gas phase, as a result of changing input parameters (initial conditions) for various cases (see Appendix A). Note that the percentage of the iodine inventory in the gas phase for IMPAIR shown in the figures does not include iodate ( $\text{IO}_3^-$ ) as an aerosol species produced by the reaction of  $\text{I}_2$  with  $\text{O}_3$ , whereas the mass balances presented in Appendix B include iodate. Note also that all of the results shown below were taken from code predictions at 25 h rather than at 75 h. This was done because at pH 5, most of the codes predicted that the iodine inventory would be almost entirely deposited on surfaces by 75 h. With only a fraction of the iodine inventory in the aqueous phase as  $\Gamma^-$ , the rate of production of volatile iodine species is much smaller at 75 h than at 25 h, and the fraction of the iodine inventory in the gas phase is significantly reduced.

##### The Effect of Dose Rate

The effect of dose rate on iodine volatility at pH 9 and pH 5, as predicted by the various codes, is shown in Figures 1 and 2.

The relationship between dose rate and iodine volatility in each of the codes is quite complex. In LIRIC and INSPECT, the dose rate affects the steady-state concentration of  $\bullet\text{OH}$ , the species responsible for the oxidation of non-volatile  $\Gamma^-$  to volatile  $\text{I}_2$ , and also affects the steady-state concentrations of  $\text{H}_2\text{O}_2$ ,  $\text{O}_2^-$  and  $e^-_{\text{aq}}$ , which reduce volatile  $\text{I}_2$  and  $\text{CH}_3\text{I}$  to non-volatile  $\Gamma^-$ . The balance between oxidant and reductant concentrations is dependent upon the pH (e.g., the  $\text{pK}_a$  of  $\text{HO}_2 = \text{H}^+ + \text{O}_2^-$  is 4.8) and the presence of impurities, such as organic compounds. The two codes are slightly different in their predictions; however, they both predict a modest (less than a factor of 10) increase in iodine volatility as the dose rate is increased by a factor of 100 at both pH values.

IODE(IPSN) and IODE(NRIR) predict that iodine volatility will increase linearly with an increase in the dose rate at pH 9. This prediction is understandable in view of the fact that IODE models the rate of production of  $\text{I}_2$  from  $\Gamma^-$  (Reaction (8)) as having a linear dependence on dose rate. In both codes, the production of organic iodides from painted surfaces has a dose rate dependence as well. Neither IODE(IPSN) nor IODE(NRIR) assumes that organic iodides are decomposed radiolytically. As a consequence, both codes predict significant increases in iodine volatility with an increase in dose rate. The results of IODE(IPSN) predictions at pH 5 are complicated by the fact that by 25 h, particularly at  $10\text{kGy}\cdot\text{h}^{-1}$ , most of the iodide in the aqueous phase has been depleted due to volatilization and adsorption, and the rate of production of volatile iodine species decreases as the amount of  $\Gamma^-$  in the aqueous phase decreases. This process results in iodine volatility at 25 h being much less than would be expected at earlier stages.

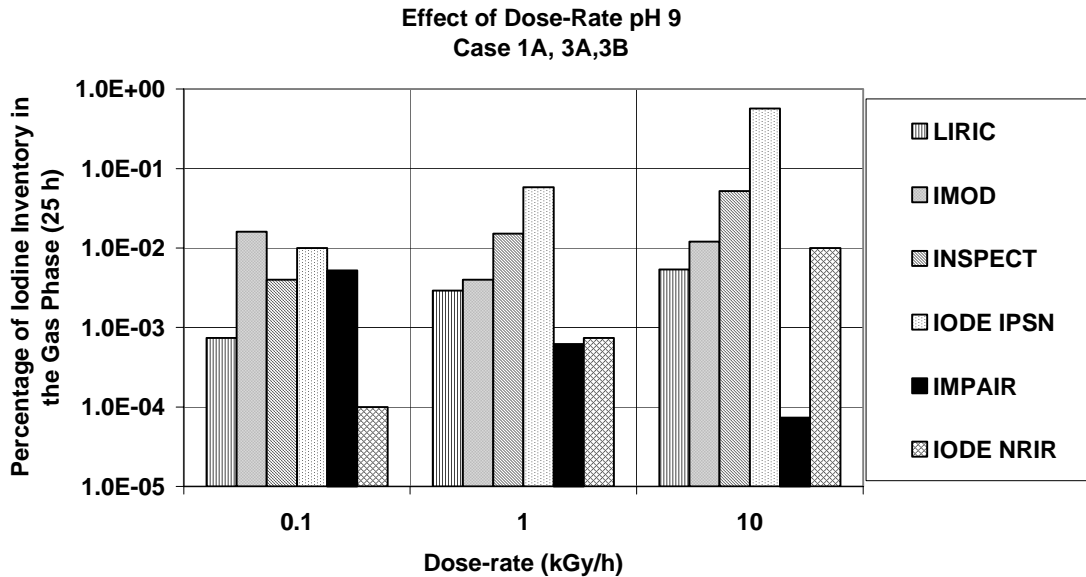


**Figure 1.** The effect of dose rate on the percentage of iodine inventory in the gas phase at 25 h for a solution initially containing  $1 \times 10^{-5} \text{ mol} \cdot \text{dm}^{-3}$  CsI at  $90^\circ\text{C}$  and pH 9.

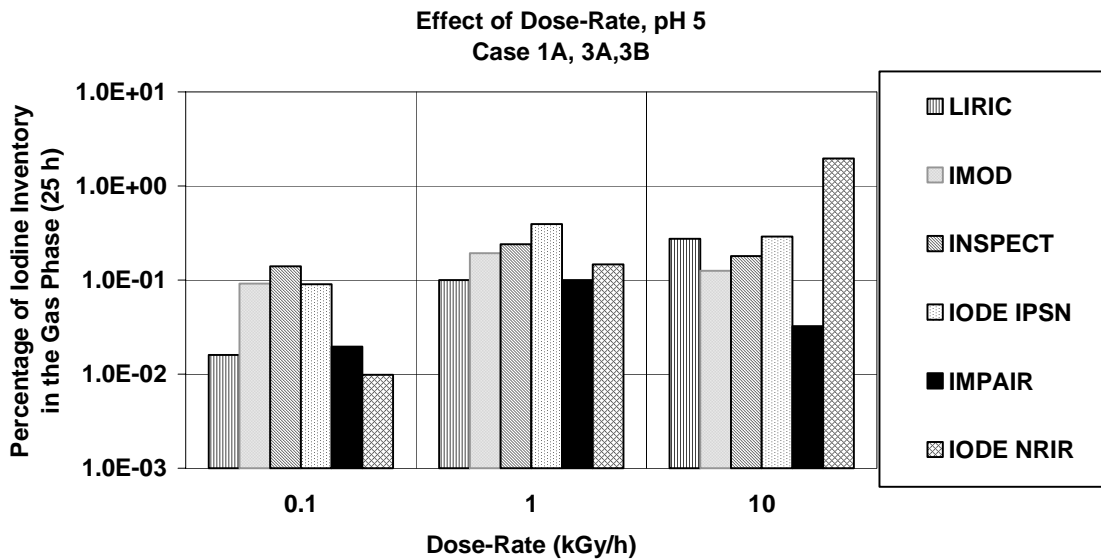


**Figure 2.** The effect of dose rate on the percentage of iodine inventory in the gas phase at 25 h for a solution initially containing  $1 \times 10^{-5} \text{ mol} \cdot \text{dm}^{-3}$  CsI at  $90^\circ\text{C}$  and pH 5.

### The Effect of pH

The pH of the aqueous phase is one of the most important factors that influences the volatility of iodine species. The effect of aqueous pH on iodine volatility at 25 h, as predicted by each of the iodine behaviour codes for aqueous solutions irradiated at 90°C and at a dose rate of 1 kGy·h<sup>-1</sup>, is shown in Figure 3.

The predicted fraction of the iodine inventory in the gas phase at 25 h, as a function of pH, varies dramatically from code to code. LIRIC and IMOD predict an increase of a factor of about 50 in iodine volatility in going from pH 9 to pH 5 (this would vary depending on the temperature), whereas IODE(IPSN) and INSPECT predict an increase of about a factor of 5 and 10, respectively. IODE(NRIR) and IMPAIR predict that iodine volatility will be higher at pH 5 than at pH 9 by a factor of about 500.

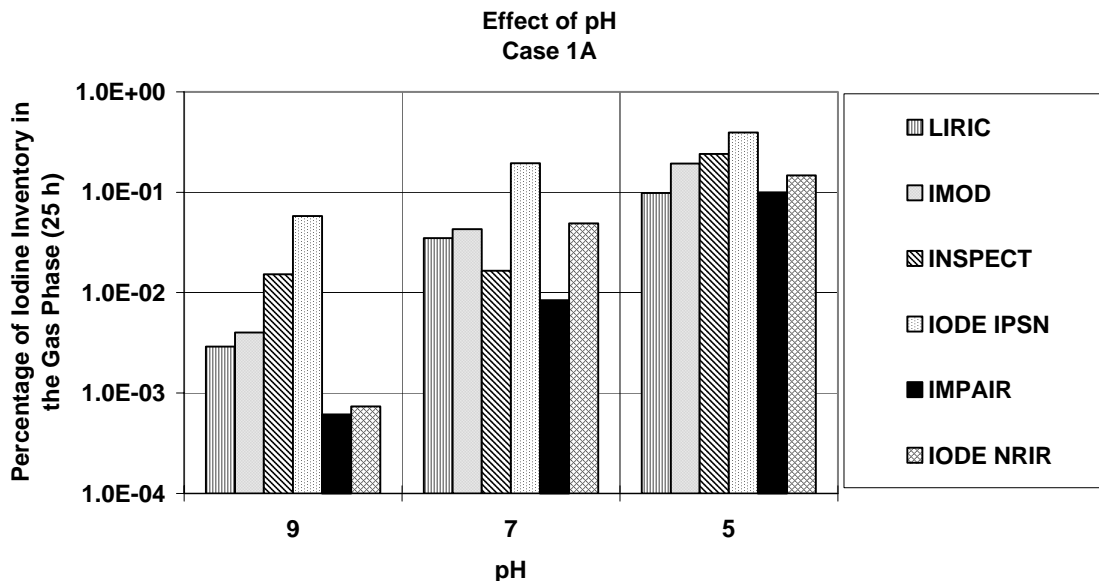


**Figure 3.** The effect of pH on the percentage of iodine inventory in the gas phase at 25 h for a solution initially containing  $1 \times 10^{-5} \text{ mol} \cdot \text{dm}^{-3}$  CsI at 90°C and irradiated at a dose rate of 1 kGy·h<sup>-1</sup>.

It is not surprising that there are some differences between the codes in their predictions of the gaseous iodine fraction at a given pH. The interconversions between non-volatile and volatile iodine species are modelled slightly differently in each code. For example, as outlined in Section 2.1, in LIRIC, IMOD and INSPECT, the rate of reduction of volatile I<sub>2</sub> and organic iodides to non-volatile I<sup>-</sup> increases with increasing pH (Reactions (1–3), (6), (7)), whereas the rate of production of I<sub>2</sub> (Reaction (5)) is pH-independent. The **overall** rate of formation of volatile iodine species as calculated by each of these codes should therefore be inversely proportional to the pH—this is what is observed. From Figure 3, there is a stronger pH

dependence in IMOD and LIRIC than in INSPECT; nevertheless, the codes are qualitatively in agreement.

In IODE(NRIR), IODE(IPSN) and IMPAIR, the rate of production of all volatile iodine species (including organic iodides) is inversely dependent on the aqueous pH (Reactions (8), (20), (22)), and the rate of decomposition of these species is pH-independent. The pH dependence of iodine volatility predicted by these codes could potentially be larger than that predicted by IMOD, LIRIC and INSPECT, because organic iodide formation has a direct pH dependence. As expected, based on the  $I_2$  and RI production rates, all the codes predict the same **overall** effect of pH on iodine volatility. Nonetheless, the sensitivity of the iodine volatility to pH changes does vary considerably, because the rate of production of  $I_2$  in each code (Reaction (8)) is defined by Equation (10), which has adjustable, user-defined parameters. The choice of parameters used in Equation (10) can substantially change the sensitivity of iodine volatility to pH.

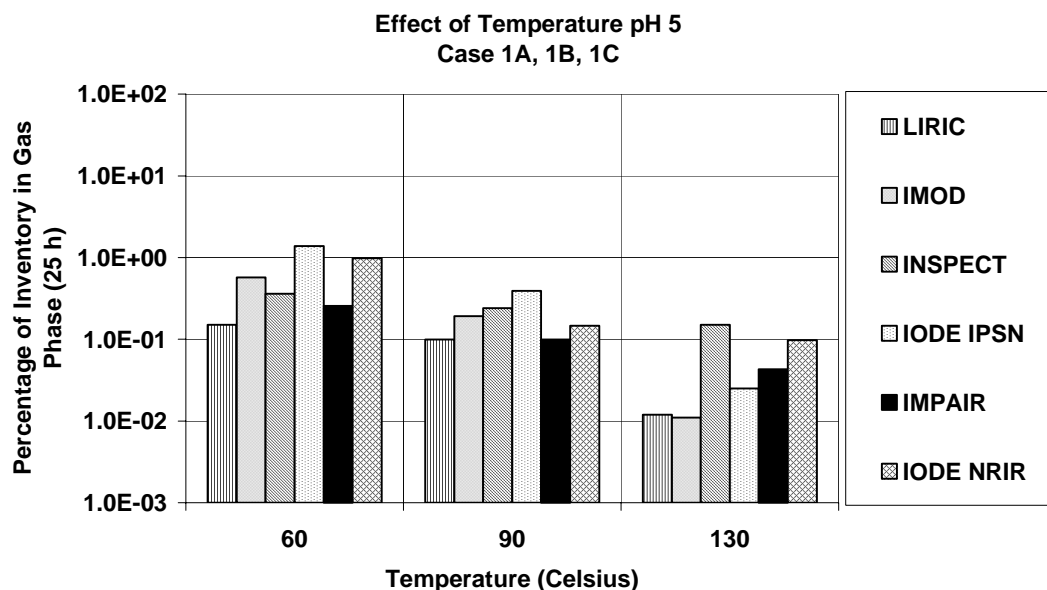


**Figure 4.** The effect of temperature on the percentage of iodine inventory in the gas phase at 25 h for a solution initially containing  $1 \times 10^{-5} \text{ mol} \cdot \text{dm}^{-3}$  CsI at pH 5 and irradiated at a dose rate of  $1 \text{ kGy} \cdot \text{h}^{-1}$ .

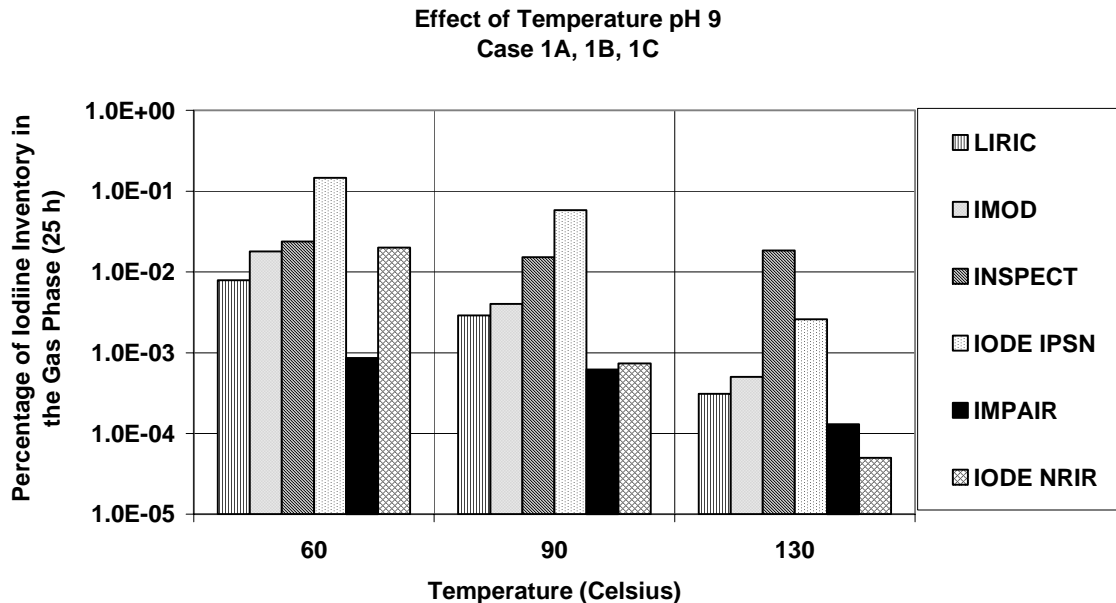


**Figure 5. The effect of temperature on the percentage of iodine inventory in the gas phase at 25 h for a solution initially containing  $1 \times 10^{-5} \text{ mol} \cdot \text{dm}^{-3}$  CsI at pH 9 and irradiated at a dose-rate of  $1 \text{ kGy} \cdot \text{h}^{-1}$ .**

#### The Effect of Temperature

The predicted effect of temperature on the fraction of the iodine inventory in the gas phase is shown in Figures 4 and 5. Most of the codes predict that an increase in temperature from 60 to 130 °C will result in a decrease in the fraction of iodine in the gas phase, both at high and low pH.

The effect of temperature on iodine volatility depends upon the balance between the temperature dependence of the production and depletion rates of volatile iodine species, and the partitioning of these species. All of the codes incorporate a temperature dependence on the partitioning of volatile iodine species, resulting in  $\text{I}_2$  and organic iodides being more volatile at higher temperatures. The recommended temperature dependence for the equilibrium-partitioning coefficient of volatile iodine species for this exercise can be found in Appendix A.

All of the codes also incorporate a temperature dependence for the iodine hydrolysis equilibrium (Reactions (1–3)) resulting in  $\text{I}_2$  being hydrolysed more rapidly to non-volatile HOI and  $\Gamma^-$  at higher temperatures. Other temperature-dependent reactions that reduce iodine volatility as temperature increases are the hydrolysis of organic iodides and the adsorption of iodine on surfaces. In general, in going from 60 to 130°C, the temperature dependence of the depletion rate of volatile iodine species more than compensates for the increase in their volatility, with the result that most of the codes predict that there will be less iodine in the gas phase at the higher temperature. INSPECT predictions at pH 9 are the exception. The temperature dependence of

Reaction (26) in INSPECT, which predicts that organic iodide production will increase with increasing temperature at about 100°C, is likely responsible for this trend.

### The Effect of Iodide Concentration

The semi-empirical codes IODE(NRIR), IODE(IPSN), IMOD and IMPAIR predict that the percentage of the iodine inventory in the gas phase is nearly independent of the initial iodide concentration, whereas LIRIC and INSPECT show a decrease in the percentage, with an increase in iodide concentration (see Figures 6 and 7). INSPECT predicts a significant (greater than a factor of 10) decrease in the percentage of iodine in the gas phase, as a result of an increase in iodide concentration by two orders of magnitude, at pH 9. At pH 5, INSPECT predicts a decrease in the gas-phase percentage as the iodide concentration is increased from  $10^{-5}$  to  $10^{-4}$  mol·dm<sup>-3</sup>, following a slight increase in iodine volatility due to an increase in iodide concentration from  $10^{-6}$  to  $10^{-5}$  mol·dm<sup>-3</sup>. LIRIC predicts a very small decrease in the gas-phase fraction as the iodide concentration is increased at pH 5, and a slightly more significant decrease at pH 9.

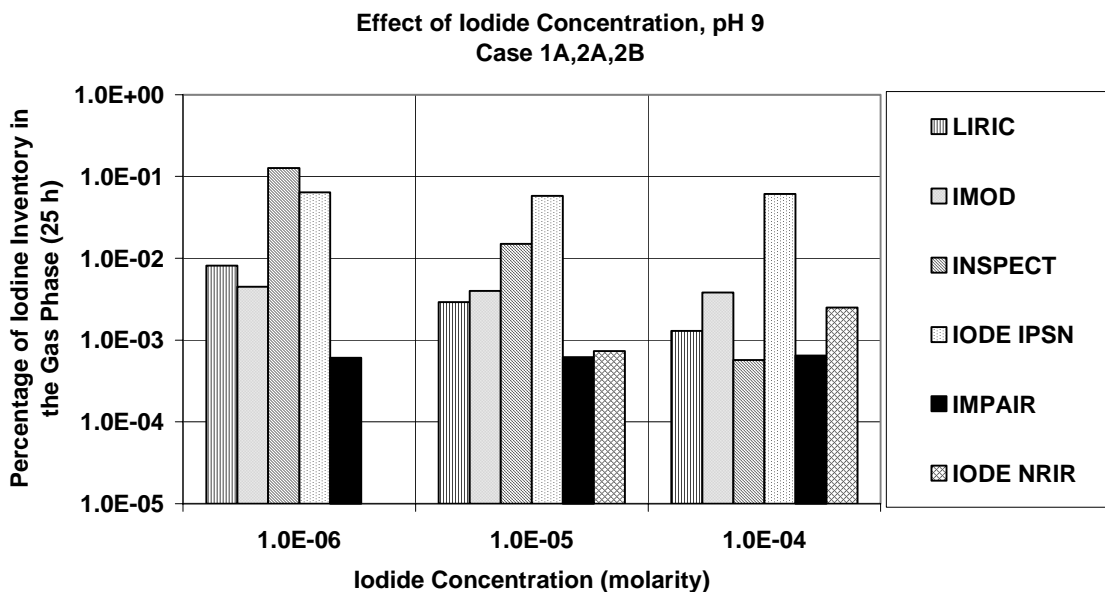


**Figure 6.** The effect of iodide concentration on the percentage of iodine inventory in the gas phase at 25 h for a solution initially containing CsI at pH 9 and 90°C irradiated at a dose rate of  $1\text{kGy}\cdot\text{h}^{-1}$ . Note that IODE(NRIR) calculations were not performed for  $1\times 10^{-6}$  mol·dm<sup>-3</sup> I<sup>-</sup>.

In IODE(NRIR), IODE(IPSN), IMOD and IMPAIR, the rate of production of I<sub>2</sub> is directly proportional to the iodide concentration (Reaction (8)). In addition, all of these codes formulate the production of organic iodides as being either directly or indirectly dependent on the iodide concentration. Therefore, regardless of whether organic iodides or I<sub>2</sub> dominates amongst gaseous

iodine species, an increase in the iodide concentration by a factor of 10 should result in all of these codes predicting about<sup>4</sup> a factor of 10 increase in the gas-phase iodine concentration—the fraction (or percentage) of the iodine inventory in the gas phase would remain unchanged. This behaviour is observed in Figure 7.

In LIRIC and INSPECT, the predicted steady-state concentration of volatile iodine species in the aqueous phase depends upon the ratio of the oxidation rate of iodide to  $I_2$  by  $\bullet OH$  radicals (Reaction (5)) to the conversion rate of  $I_2$  and RI to non-volatile species by hydrolysis and radiolysis ((Reactions (1–3), (6), (7), (17), (18))). These codes differ from the semi-empirical codes, in that an increase in  $\Gamma$  concentration does not result in a proportional increase in the rate of production of  $I_2$ , because an increase in  $\Gamma$  concentration also serves to decrease the steady-state concentration of  $\bullet OH$ , i.e., the species responsible for oxidizing iodide to  $I_2$ .<sup>5</sup> Based on the rate of formation of  $I_2$  alone, an increase in iodide concentration by a factor of ten would result in less than a factor of ten increase in the concentration of  $I_2$  in the aqueous or gas phase, and a small decrease in the percentage of iodine inventory in the gas phase.

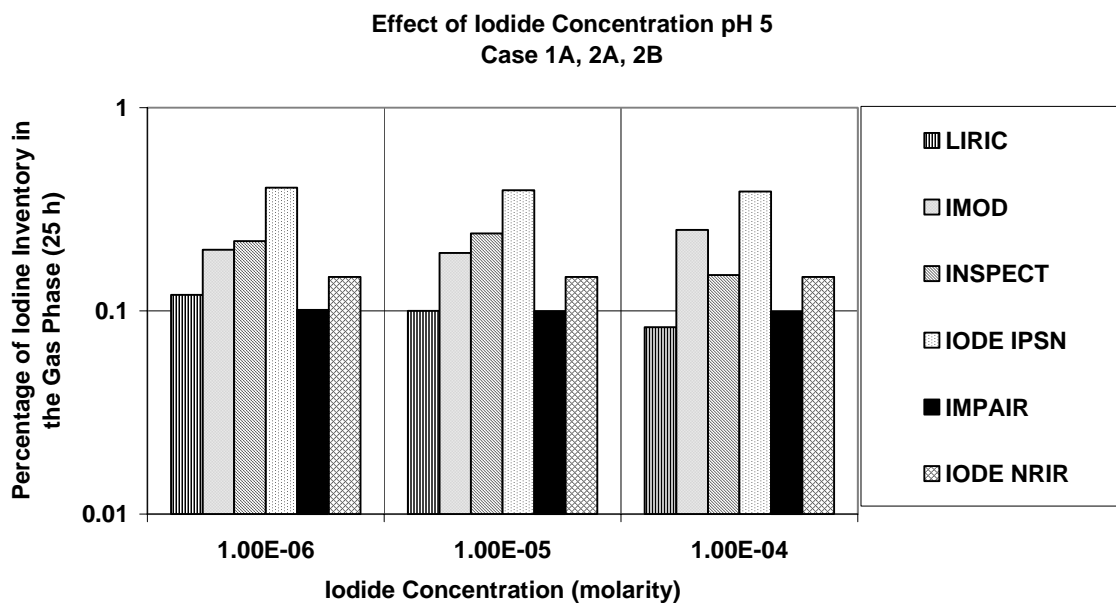


**Figure 7. The effect of iodide concentration on the percentage of iodine inventory in the gas phase at 25 h for a solution initially containing CsI at pH 5 and 90°C irradiated at a dose rate of 1 kGy·h<sup>-1</sup>.**

<sup>4</sup> A small dependence of the percentage on the initial iodide concentration may be observed in these codes, if the contribution of the iodine hydrolysis equilibrium (Reaction (1)) to the conversion of non-volatile iodine species to  $I_2$  is significant.

<sup>5</sup> At 1 kGy·h<sup>-1</sup>, the steady-state concentration of  $\bullet OH$  is significantly decreased, when iodide concentrations approach about  $10^{-4}$  mol·dm<sup>-3</sup>. Also, the  $\bullet OH$  concentration is decreased by the presence of organic impurities. Therefore, the overall rate of production of  $I_2$  may not increase linearly with an increase in iodide concentration.

In LIRIC and INSPECT, the depletion of  $I_2$  in the aqueous phase is also dependent upon iodide concentration. The hydrolysis equilibrium (Reaction (1)) dictates that an increase in iodide concentration decreases the rate of depletion of  $I_2$  by hydrolysis, and increases iodine volatility. The depletion of  $I_2$  by  $O_2^-$  (Reaction (6)) has the opposite iodide dependence, because an increase in iodide concentration increases the  $O_2^-$  concentration. For LIRIC and INSPECT predictions under acidic or neutral (pH 4-7) conditions, the iodide dependence of the hydrolysis equilibrium offsets the dependence of the rate of formation of  $I_2$ ; the codes predict that the gaseous iodine fraction changes only slightly with iodide concentration. At high pH values, however, the iodine hydrolysis equilibrium (Reaction (3)) lies so far to the right (i.e., it favours the formation of  $I^-$  and HOI), that it becomes virtually independent of iodide concentration. At pH 9, the iodide dependence of the percentage of iodine inventory in the gas phase is what would be expected based on the dependence of the  $I_2$  formation rate on iodide concentration. This iodide dependence is further augmented by the iodide dependence of  $O_2^-$  reduction. Therefore, at pH 9 and 90°C, LIRIC and INSPECT predict that an increase in iodide concentration will more substantially decrease the percentage of the iodine inventory in the gas phase.

### The Effect of Condensation

The effect of condensation on iodine volatility at pH 5, as predicted by each of the codes, is shown in Figure 8. IMPAIR, LIRIC and IMOD predict that the presence of condensing steam will increase iodine volatility, whereas INSPECT, IODE(IPSN) and IODE(NRIR) predict that it will decrease the gaseous iodine fraction. The qualitative predictions of each of the codes at pH 9 are the same as for pH 5.

Code predictions regarding the effect of condensing steam on iodine volatility depend on whether the rates for removal of airborne iodine by condensation (i.e., absorption into the condensate, and return flow to the sump) are faster or slower than the rates of removal of iodine by absorption onto surfaces in the absence of condensation. In LIRIC, IMOD and IMPAIR, the default rate constants for the removal of iodine from the gas phase are such that iodine is removed more slowly in the presence of condensation than under dry conditions. That is, the overall rate for the deposition of iodine, which encompasses absorption into a condensing film, and absorption onto surfaces in contact with the condensing film, is lower than the rate constant for deposition onto dry surfaces. As a result, these codes predict that less iodine is lost to the surfaces in the presence of condensing steam, and that the gaseous fraction increases. On the other hand, IODE(IPSN), IODE(NRIR) and INSPECT predict that the rate of removal of gaseous iodine species to the surfaces is enhanced by condensation, because this process enhances the mass flux to the surface. As a result, these codes predict a decrease in iodine volatility as a result of condensation. Note that the effect is quite small for all of the codes.

---

<sup>6</sup> At 1 kGy·h<sup>-1</sup>, the steady-state concentration of •OH is significantly decreased, when iodide concentrations approach about 10<sup>-4</sup> mol·dm<sup>-3</sup>. Also, the •OH concentration is decreased by the presence of organic impurities. Therefore, the overall rate of production of  $I_2$  may not increase linearly with an increase in iodide concentration.



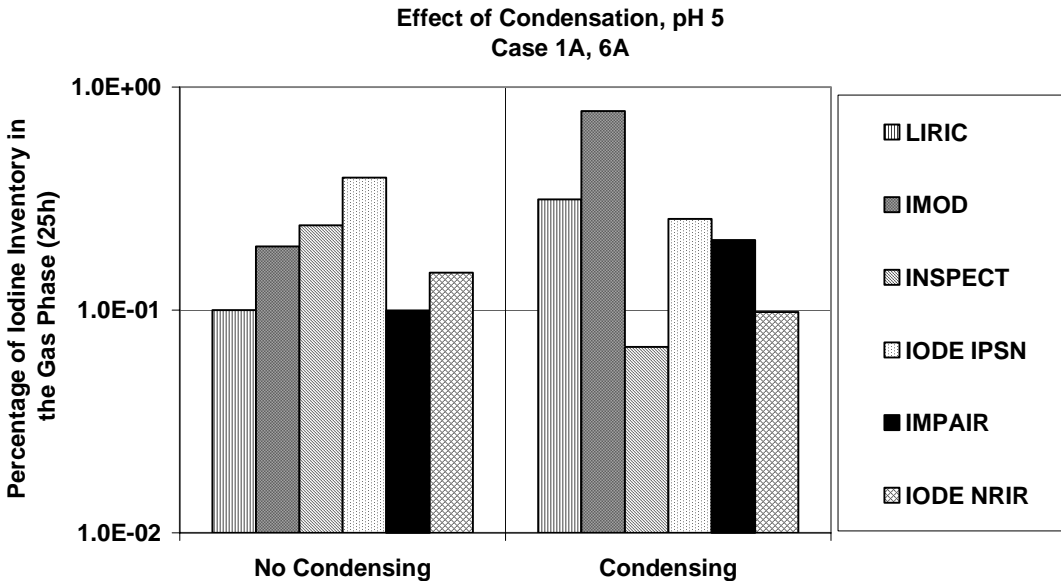


**Figure 8.** The predicted effect of condensing steam on the percentage of iodine inventory in the gas phase at 25 h for a solution initially containing  $1 \times 10^{-5} \text{ mol} \cdot \text{dm}^{-3}$  CsI at pH 5 and  $90^\circ\text{C}$  irradiated at a dose rate of  $1 \text{ kGy} \cdot \text{h}^{-1}$ .

#### The Effect of Silver

The effect of the presence of silver in the sump, as predicted by each of the codes, is shown in Figure 9.

As would be expected, all of the codes predict that iodine volatility is reduced when silver is present. However, the magnitude of the decrease in volatility varies quite dramatically. For the conditions used in Figure 9, for example, IMPAIR predicts that the presence of silver would reduce iodine volatility almost imperceptibly, whereas in IODE(IPSN), the predicted amount of iodine in the gas phase is reduced by four orders of magnitude.

Some of the differences between code predictions can be attributed to the different mechanisms that are assumed for iodine adsorption on Ag. For example, both IODE(IPSN) and INSPECT assume that AgO reacts with  $\Gamma$ , with AgO being formed from Ag in a pH-dependent process. LIRIC, IMOD and IODE(NRIR), on the other hand, assume that only  $\text{I}_2$  reacts with Ag. However, the effect of Ag on iodine volatility is also dependent upon the amount of various iodine species calculated by each code. IODE(IPSN) and INSPECT both assume that iodide reacts with AgO (Reaction (30b)) and that  $\text{I}_2$  reacts with Ag (Reaction (28)). These codes use the same rate constants for reactions between silver species and iodine species, yet their predictions of iodine volatility in the presence of Ag are quite different. This discrepancy occurs because the codes differ in their predictions regarding the rates of formation and destruction of  $\text{I}_2$  (Reactions (5) and (8)), the processes that determine the concentrations of  $\text{I}_2$  and  $\Gamma$  that will be reacting with silver species.

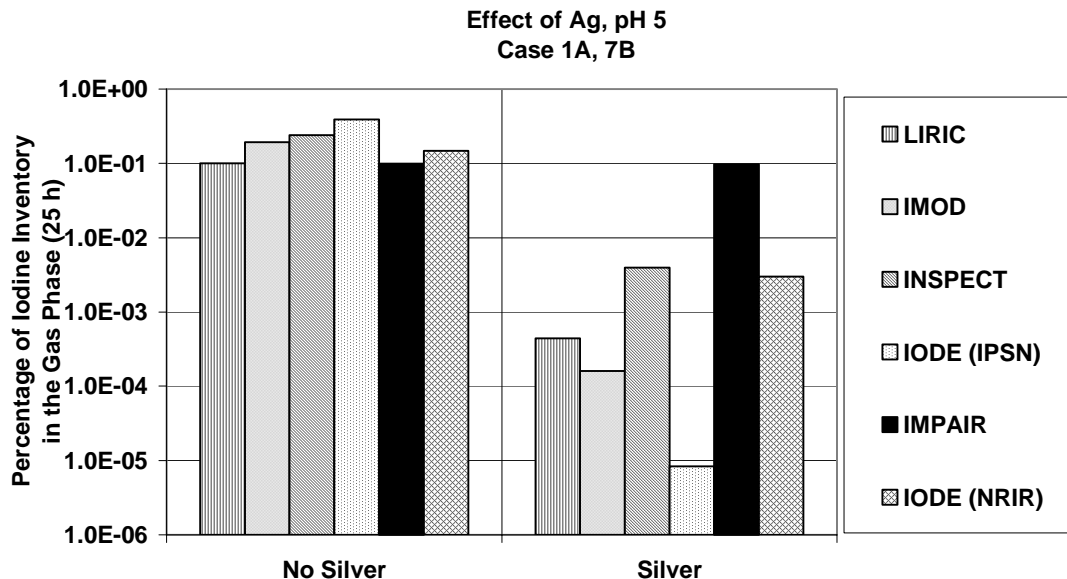


**Figure 9.** The predicted effect of Ag in the aqueous phase on the percentage of iodine inventory in the gas phase at 25 h for a solution initially containing  $1 \times 10^{-5} \text{ mol} \cdot \text{dm}^{-3}$  CsI at pH 5 and  $90^\circ\text{C}$  irradiated at a dose rate of  $1 \text{ kGy} \cdot \text{h}^{-1}$ .

IMPAIR predicts that Ag will have a negligible impact on iodine volatility for three reasons. Firstly, in IMPAIR,  $\text{I}_2$  is converted rapidly to  $\text{IO}_3^-$  in the gas phase; a much smaller fraction of iodine is present in the aqueous phase (as  $\text{I}_2$ ) than in the other codes. Secondly, the rate constant used for the reaction between  $\text{I}_2$  and Ag is smaller in IMPAIR ( $2.2 \times 10^{-6} \text{ m} \cdot \text{s}^{-1}$ ) than in IODE, IMOD and LIRIC ( $1 \times 10^{-5} \text{ m} \cdot \text{s}^{-1}$ ). Finally, IMPAIR does not consider  $\text{Ag}_2\text{O}$  as a reactive species, and assumes that Ag reacts with  $\text{I}^-$  at a relatively slow rate. ( $2.2 \times 10^{-6} \text{ m} \cdot \text{s}^{-1}$ ). Consequently, much less of the iodine inventory is retained by Ag in IMPAIR, and the gaseous iodine fraction is not influenced as much by the presence of Ag as it is in the other codes.

#### The Effect of Organic Impurity Concentrations

The effect of an initial organic impurity concentration on the iodine volatility predicted by each code is shown in Figure 10. Note that the calculations presented in Figure 10 for IODE(NRIR) for  $1 \times 10^{-3} \text{ mol} \cdot \text{dm}^{-3}$  organic impurity are the same as the calculations of these codes for Case 1A, in which the organic impurity concentration is user-defined. IODE(NRIR) already assumes an initial organic impurity level of about  $1 \times 10^{-3} \text{ mol} \cdot \text{dm}^{-3}$ ; therefore, the conditions used to generate Figure 10 are qualitatively the same as those used for Case 1A. There are no INSPECT calculations for this case, because INSPECT does not include a homogeneous aqueous-phase mechanism for the formation of organic iodides.

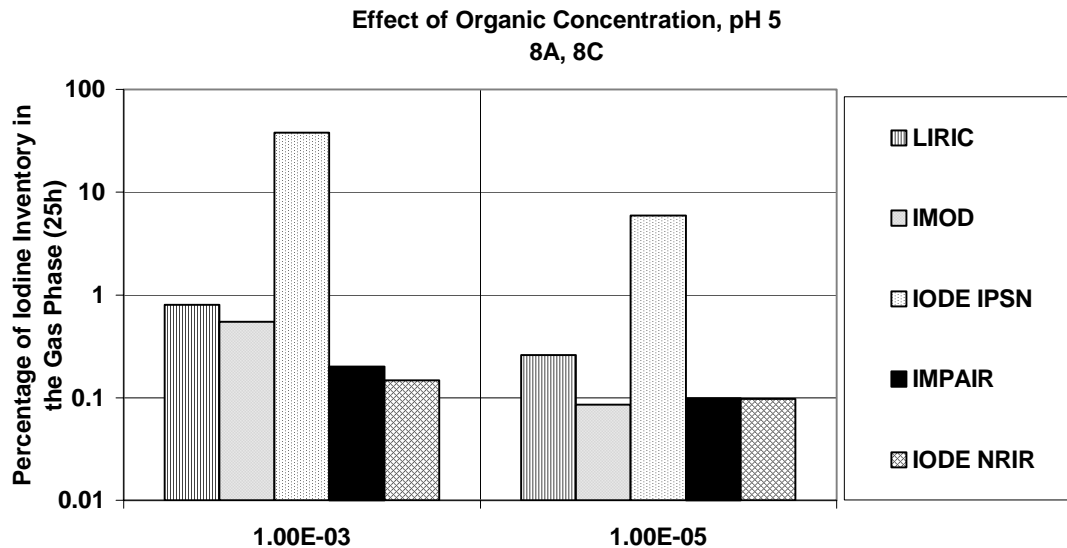


**Figure 10. The predicted effect of organic impurities in the aqueous phase on the percentage of iodine inventory in the gas phase at 25 h for a solution initially containing  $1 \times 10^{-5} \text{ mol} \cdot \text{dm}^{-3}$  CsI at pH 5 and  $90^\circ\text{C}$  irradiated at a dose rate of  $1 \text{ kGy} \cdot \text{h}^{-1}$ .**

In general, the codes predict that an increase in organic impurity concentration results in an increase in the amount of iodine in the gas phase. This can be rationalized in view of the fact that the rate of production of organic iodides from homogeneous aqueous-phase processes (Reactions (16) and (20)) is dependent upon the concentration of organic radicals in the aqueous phase, and this concentration should, in turn, be dependent upon the concentration of organic impurities in the sump. In all of the codes, organic iodide production by homogeneous aqueous-phase processes results in only a small fraction of the  $\text{I}_2$  produced being converted to organic iodides, and  $\text{I}_2$  is the dominant volatile species that is produced. However,  $\text{I}_2$  is easily absorbed on surfaces, whereas organic iodides are not. Once partitioned into the gas phase, organic iodides persist as volatile species, whereas  $\text{I}_2$  is rapidly removed by absorption. As a result, most of the codes predict that a large fraction of the gaseous iodine inventory is in the form of organic iodides, and the total iodine concentration in the gas phase is dependent on the rate of the organic iodide formation in the aqueous phase.

### pH Predictions

Only LIRIC, IMOD and IODE(IPSN) have the option of performing calculations to model pH behaviour in unbuffered solutions. An example of the predictions of each of the codes is shown in Figure 11 for a solution containing  $1 \times 10^{-5} \text{ mol} \cdot \text{dm}^{-3}$  CsI at  $90^\circ\text{C}$ , irradiated at a dose rate of  $10 \text{ kGy} \cdot \text{h}^{-1}$ .

## CASE 5B

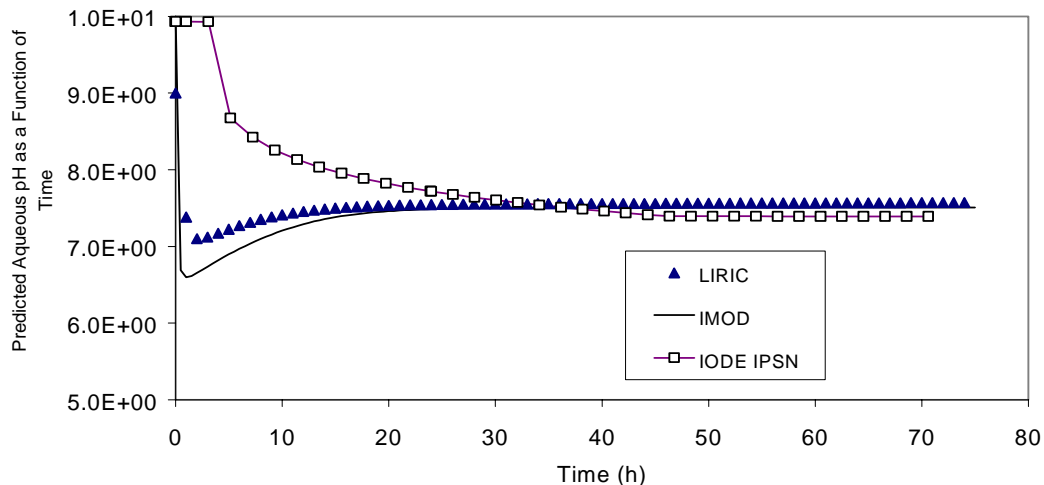


**Figure 11.** The pH of irradiated ( $10 \text{ kGy}\cdot\text{h}^{-1}$ ) containment sump water initially containing  $1 \times 10^{-5} \text{ mol}\cdot\text{dm}^{-3}$  CsI at pH 5 and at  $90^\circ\text{C}$  as predicted by LIRIC, IMOD, and IODE(IPSIN). The sump water is assumed to be in contact with painted surfaces.

As would be expected, LIRIC and IMOD predict very similar pH profiles. The reactions and rate constants that induce pH changes (i.e., the release of organic compounds into the aqueous phase (Reaction (19)) and their subsequent radiolytic decomposition (Reactions (14), (15))) in these models are virtually identical. IODE(IPSIN) predicts a more modest rate of decrease in aqueous pH initially, because the pH model in IODE(IPSIN) takes into account the buffering effects of boron released from safety systems and  $\text{CO}_2$  release from MCCI as well as the formation of nitric acid from air and ozone interaction. The final pH value predicted by IODE(IPSIN) is similar to that obtained by LIRIC and IMOD, because a buffering effect of  $\text{CO}_2$  is predicted by all codes. Results obtained using dose rates of  $1 \text{ kGy}\cdot\text{h}^{-1}$  and  $0.1 \text{ kGy}\cdot\text{h}^{-1}$  are qualitatively similar; the radiolysis of organic materials to organic acids as modelled by LIRIC and IMOD has a greater impact on aqueous pH than does the cumulative effect of nitric acid formation and the release of  $\text{CO}_2$  from the MCCI in IODE(IPSIN).

#### Effect of a Programmed pH Drop

Figure 12 shows the effect of rapidly decreasing pH on iodine volatility, as predicted by each of the codes. Most of the codes predict similar kinetic behaviour, with the gas-phase iodine concentration increasing rapidly as the pH decreases. The gas-phase iodine concentration is also, in most cases, predicted to reach a maximum value, followed by a slow decrease as  $\text{I}_2$  is adsorbed on surfaces. The strange behaviour of the gas-phase concentration predicted by LIRIC is an artefact of the way in which the pH values were provided as input.

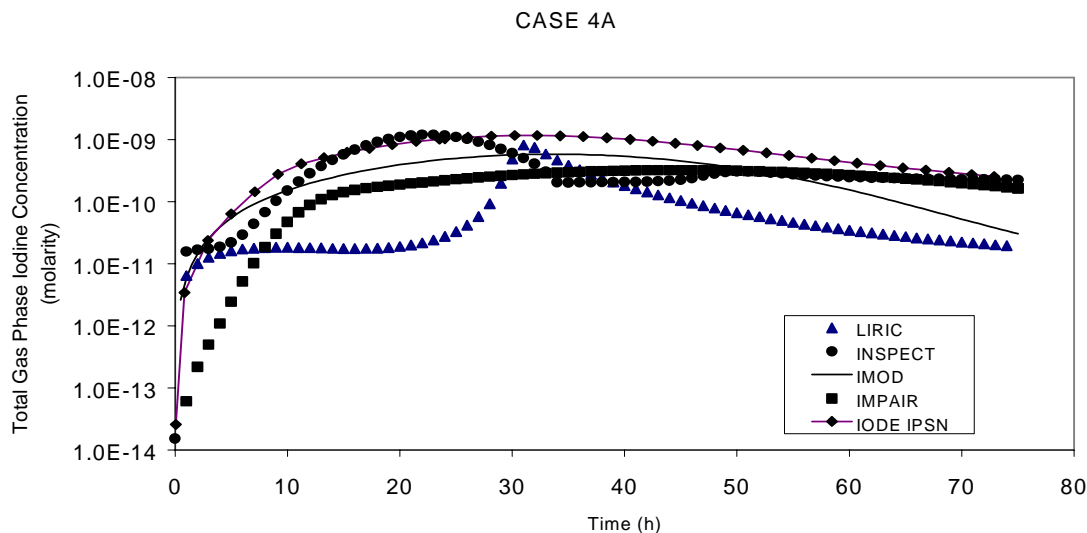


**Figure 12.** The total iodine concentration in the gas phase from an irradiated ( $1 \text{ kGy}\cdot\text{h}^{-1}$ ) solution initially containing  $1\times 10^{-5} \text{ mol}\cdot\text{dm}^{-3}$  CsI and at  $90^\circ\text{C}$ , as predicted by the iodine behaviour codes. The pH is assumed to start at 10, and then drop to around 3.5 in 75 h.

FACSIMILE<sup>7</sup>, the commercial differential equation solver used to solve the kinetics of the reactions described in LIRIC, uses an integration method that assumes that variables are smooth functions over time, and estimates a polynomial approximation for the values of the variables over a large integration step. When one introduces a large step change in one variable or parameter (e.g., a pH drop from 10 to 9.5), the FACSIMILE approximation for changes in the concentration of other variables (e.g., water radiolysis product concentrations) is less accurate than when only small changes in input parameters are made. The application of several consecutive large perturbations to the pH values results in a significant time lag between the pH being changed and the  $\text{I}_2$  concentrations responding to the change. This effect can be seen in Figure 13. When a pH change is input every  $\frac{1}{2}$  h, the gaseous iodine concentration remains the same for the first 20 h, even though the pH drops significantly over the same time period. As the pH input is increased in frequency, and the pH steps become smaller, the amount of time required for species concentrations to reach a steady state decreases, and the time lag between a pH change and an increase in iodine volatility gets progressively smaller. Presumably, if the pH was provided as input every second or fraction of a second, then a smooth concentration profile would be observed for the gaseous iodine concentration, similar to that predicted by the other models.

<sup>7</sup> The FACSIMILE program is a commercial integration package (AEA Technologies, Harwell, UK) for solving coupled-differential equations that was specifically designed for chemical systems. The chemical system to be modelled is expressed as a series of simple chemical reactions, which is then converted into coupled differential equations and solved by FACSIMILE's numerical integration method.

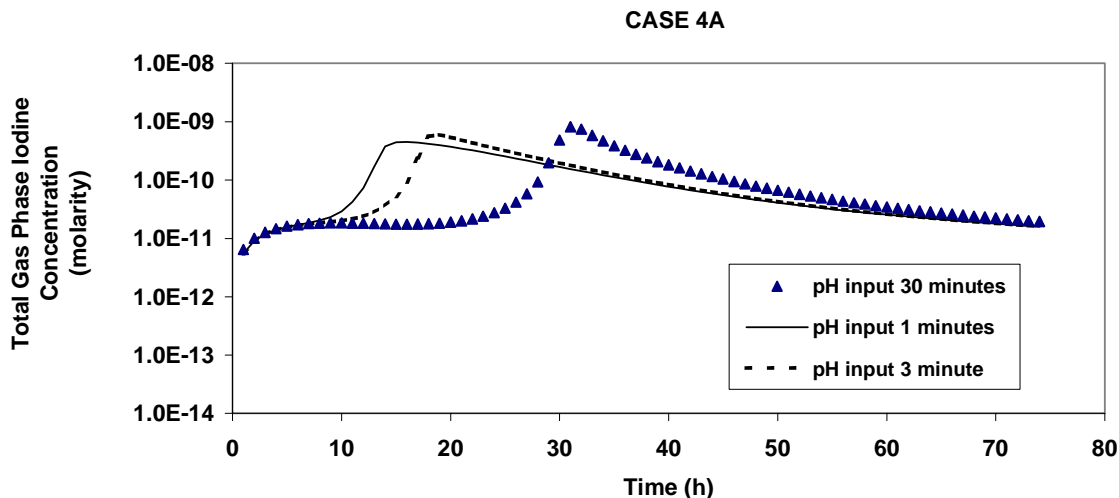


**Figure 13. Predicted concentration of iodine species in the gas phase from a containment sump initially containing  $1 \times 10^{-5} \text{ mol} \cdot \text{dm}^{-3}$  CsI solution ( $1 \text{ kGy} \cdot \text{h}^{-1}$ ,  $90^\circ\text{C}$ ). The pH is assumed to start at 10, and then drop to around 3.5. The effect of various time steps for pH input is shown.**

The LIRIC results shown in Figure 13 are a clear demonstration that care must be taken in the way in which user-defined input is provided to models. To have confidence in model predictions, the responses of the model to input parameters and the form in which the parameters are introduced must be well understood. Note that the problem with the predictions presented in Figure 13 derive from the fact that the input provided to the model did not provide a sufficiently accurate description of the pH profile. The problem is an artefact of the solver, and not of the LIRIC model itself. A comparison of LIRIC predictions with experimental data obtained in intermediate-scale studies indicates that LIRIC also models the effect of real stepwise pH changes on iodine volatility very well [3]. Intermediate-scale studies have also shown that LIRIC performs well when changes in pH are calculated within the model (as a result of organic radiolysis, for example), rather than imposed externally [3].

### 3.2 General Observations

The agreement between code predictions for various cases ranges from excellent to poor. For example, a plot of the predicted concentration of iodine in the gas phase for the boundary conditions corresponding to Case 1A, pH 5 ( $1 \times 10^{-5} \text{ mol} \cdot \text{dm}^{-3}$  CsI at  $90^\circ\text{C}$ , irradiated at a dose rate of  $1 \text{ kGy} \cdot \text{h}^{-1}$  and in the absence of condensing steam) are shown in Figure 14. The code predictions in the figure (with the exception of IMPAIR predictions including iodate) are very similar, with the calculated gaseous iodine fraction varying less than an order of magnitude from code to code. In contrast, Figure 15 shows case 8A, pH 5, in which the conditions are identical to Case 1A, pH 5, with the exception that there is  $1 \times 10^{-3} \text{ mol} \cdot \text{dm}^{-3}$  organic impurities initially in

the aqueous phase. For this case, the code predictions of the gaseous iodine inventory vary by almost three orders of magnitude.

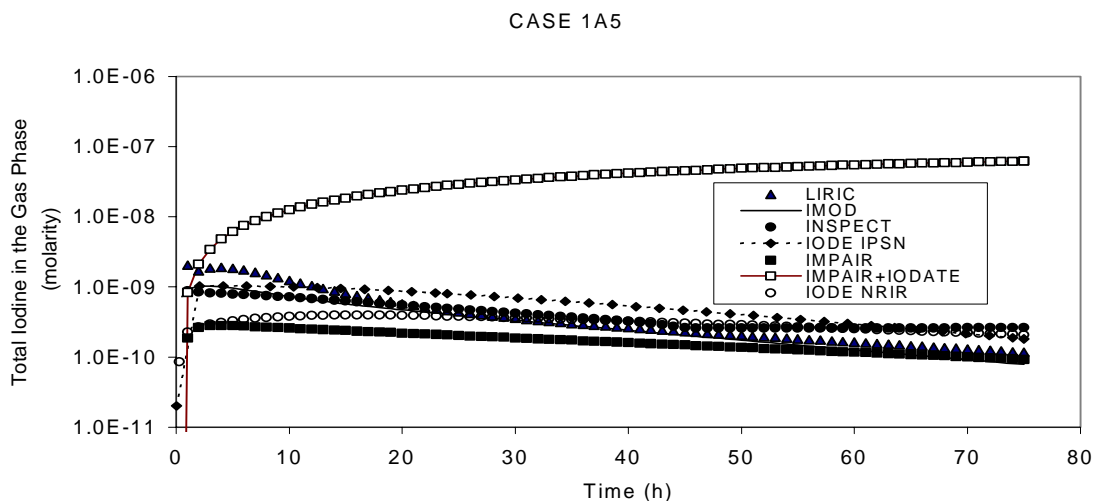


**Figure 14.** The total iodine concentration in the gas phase from an irradiated ( $1 \text{ kGy}\cdot\text{h}^{-1}$ ) solution initially containing  $1 \times 10^{-5} \text{ mol}\cdot\text{dm}^{-3}$  CsI at pH 5 and at  $90^\circ\text{C}$ , as predicted by the iodine behaviour codes. The sump water was assumed to be in contact with painted surfaces.

The extent to which the code predictions agree with one another varies from case to case; however, it appears that the worst agreement occurs at high dose rates, high temperature ( $130^\circ\text{C}$ ), high iodide concentration, and in the presence of large quantities of organic impurities.

In general, IMPAIR predicts a smaller gas-phase fraction than the other codes. The low values predicted by IMPAIR for the fraction of iodine in the gas phase is the result of molecular iodine being depleted in the gas phase by its reaction with  $\text{O}_3$  to produce iodate. This extra decomposition path contributes to smaller  $\text{I}_2$  concentrations in the gas and aqueous phase. Note, in Figure 14, that the gas-phase concentration, if  $\text{IO}_3^-$  is considered, is almost three orders of magnitude larger than if only  $\text{I}_2$  and  $\text{CH}_3\text{I}$  are considered.

One of the most noticeable differences between the code calculations for every case is the fraction of iodine in the gas phase in the form of organic iodides. The organic iodide formation models in each code are quite different (with various dose rate, iodide and temperature dependences), and this fact is largely responsible for discrepancies between predictions of the overall gaseous iodine fractions, such as those observed in Figure 16. The organic iodide fraction at 75 h for case 1A, in which the iodide concentration was  $1 \times 10^{-5} \text{ mol}\cdot\text{dm}^{-3}$ , the temperature was  $90^\circ\text{C}$  and the dose rate was  $1 \text{ kGy}\cdot\text{h}^{-1}$ , are shown in Table 1. Figure 16 shows a comparison of the amount of organic iodides in the gas phase as a function of time, under the same conditions as the calculations shown in Figure 14.

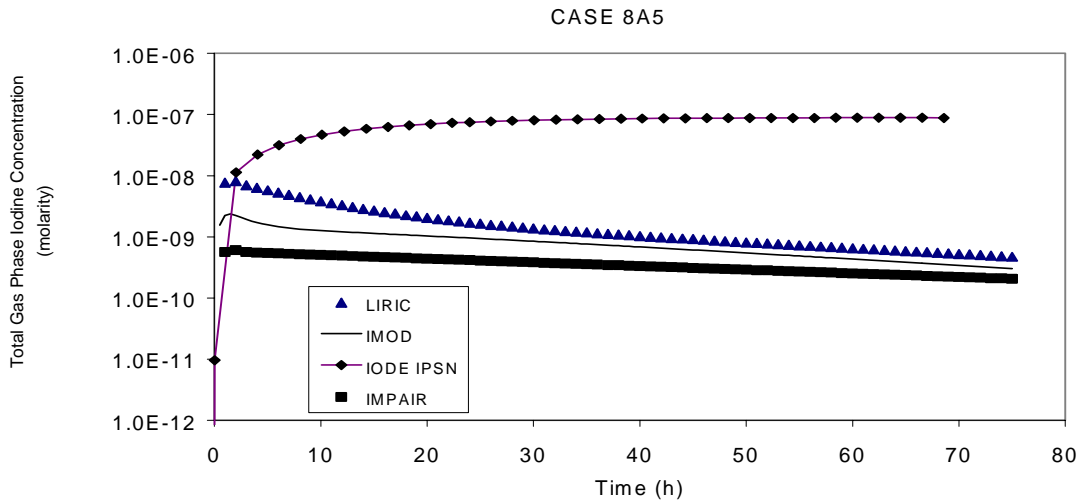


**Figure 15.** The total iodine concentration in the gas phase from an irradiated ( $1 \text{ kGy}\cdot\text{h}^{-1}$ ) solution initially containing  $1\times 10^{-5} \text{ mol}\cdot\text{dm}^{-3}$  CsI at pH 5 and at  $90^\circ\text{C}$ , as predicted by the iodine behaviour codes. Organic impurities initially in the sump are assumed to be  $1\times 10^{-3} \text{ mol}\cdot\text{dm}^{-3}$ .

A comparison of Figures 14 and 16 demonstrates that even when the iodine behaviour codes give very good quantitative agreement regarding the total amount of iodine in the gas phase, the percentage of the total iodine inventory in the form of gaseous organic iodides differs considerably. The variation in the amount of organic iodide predicted to be in the gas phase is also demonstrated by Table 1. The predicted percentages of organic iodides for Case 1A pH5 vary by two orders of magnitude between the codes.

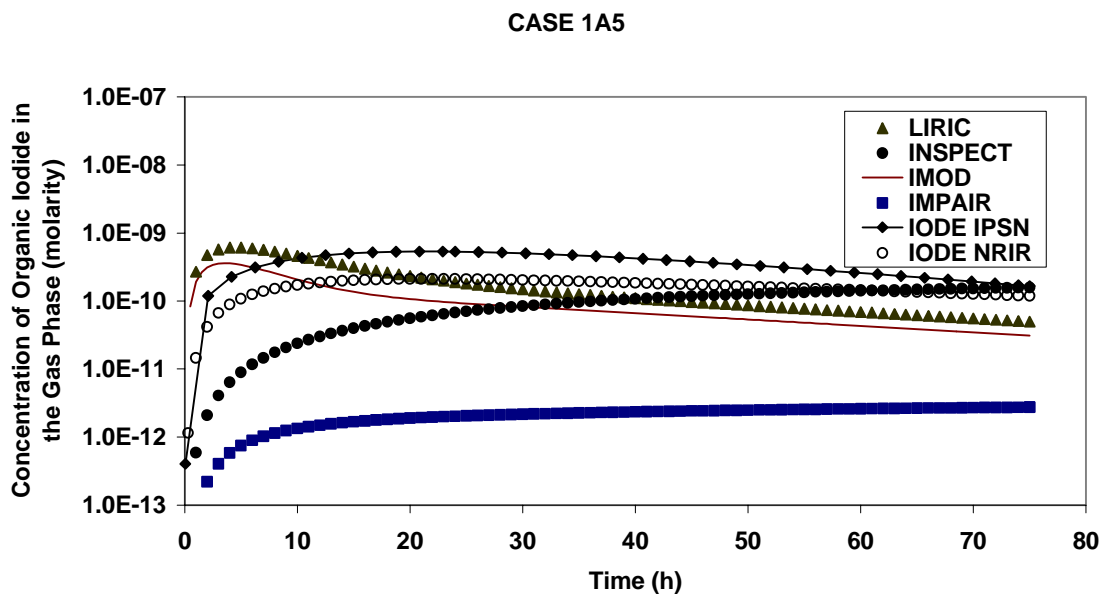




**Figure 16.** The organic iodide concentration in the gas phase from an irradiated ( $1\text{kGy}\cdot\text{h}^{-1}$ ) solution initially containing  $1\times 10^{-5}\text{ mol}\cdot\text{dm}^{-3}$  CsI at pH 5 and at  $90^{\circ}\text{C}$ , as predicted by the iodine behaviour codes. The sump water was assumed to be in contact with painted surfaces.

**Table 1.** Predicted percentage of the total iodine inventory in the form of gaseous organic iodides in case 1A at 75 h.

pH	LIRIC	IMOD	INSPECT	IODE IPSN	IODE NRIR	IMPAIR
9	$1.6\times 10^{-3}$	$3.9\times 10^{-4}$	$1.8\times 10^{-2}$	$9\times 10^{-2}$	$2.2\times 10^{-4}$	$5.3\times 10^{-3}$
5	$2.4\times 10^{-2}$	$1.5\times 10^{-2}$	$1.1\times 10^{-1}$	$8.2\times 10^{-2}$	$1.2\times 10^{-1}$	$1.3\times 10^{-3}$